MULTI-TEMPORAL SAR METRICS APPLIED TO MAP WATER BODIES

Maurizio Santoro, Urs Wegmüller

Gamma Remote Sensing, Gümligen, Switzerland
http://www.gamma-rs.ch; E-mail: santoro@gamma-rs.ch

ABSTRACT

Multi-temporal synthetic aperture radar (SAR) metrics are investigated to assess their capability for mapping land cover types. The temporal variability and the minimum backscatter in a time series of Envisat Advanced SAR (ASAR) Wide Swath Mode (WSM) backscatter measurements present unique features over water surfaces with respect to other land cover types. A simple thresholding algorithm applied to these metrics is then presented to detect water bodies. Results from six study areas in Europe and Central Siberia show consistency of the behavior of the multi-temporal metrics over "water" and "land" areas regardless of the specific region. Water body detection accuracies are mostly above 90%, omissions occurring when a water body has a size similar to the pixel size of the SAR image.

Index Terms— Envisat ASAR, Wide Swath Mode, water bodies, multi-temporal, backscatter

1. INTRODUCTION

Detection of water bodies with synthetic aperture radar (SAR) data is typically achieved by exploiting the very low backscattered intensity [1] or interferometric coherence [2]. Both observables have however limitations because other land cover classes might present similar signatures or the signal is not stable in time depending on the water surface conditions. At C-band (wavelength: 5.6 cm) and for co-polarized data, the very high temporal variability of the signal over water and the frequently very low backscatter are however unique with respect to other land cover classes. In this paper, we report on a signature analysis of multi-temporal SAR metrics for different land cover classes and devise a simple algorithm for the detection of water bodies with respect to land surfaces.

2. SAR DATA AND STUDY AREAS

To devise the capability of multi-temporal SAR metrics for detection of water bodies, Envisat Advanced SAR (ASAR) Wide Swath Mode (WSM) data were considered. Because of the strong swath overlap, a large number of backscatter observations become available within a short period of time. In addition, Envisat ASAR WSM data are acquired repeatedly on a global scale so that they are suitable if an application based on multi-temporal data on a global scale is aimed at.

Six study areas in Europe and Central Siberia were considered (Table 1), with different types of water bodies and land surfaces. For each, ASAR WSM data acquired during 2005 were considered. The SAR data have been multi-looked, terrain geocoded [3] and speckle filtered with a multi-channel filter [4]. Normalization of the backscatter for slope induced effects was then applied [5]. The original detected WSM images (pixel size: 75m; spatial resolution: 150 m) were processed to 75, 150 and 300 m pixel size with multi-look factors of 1×1, 2×2 and 4×4 to investigate the effect of spatial resolution.

For each SAR dataset, the corresponding average backscatter, the minimum backscatter of a time series and the temporal variability, i.e., the standard deviation of the backscatter, were computed. Figure 1 shows a false color composite of the three multi-temporal SAR metrics (red: average SAR backscatter; green: minimum SAR backscatter; blue: temporal variability of SAR backscatter) for the Netherlands. Water surfaces appear as blue because of the highest temporal variability and lowest minimum backscatter when compared to other land surfaces. Land surfaces are characterized by a low contribution of the blue component related to the temporal variability instead. Similar features were obtained for all study areas listed in Table 1.

Table 1. Study areas and number of ASAR Wide Swath Mode images available for the year 2005.

Study area	Number of ASAR images
Västerbotten, Sweden	146
Andalusia, Spain	86
The Netherlands	95
Switzerland	53
Northern Poland	160
Krasnoyarsk Region, Russia	133

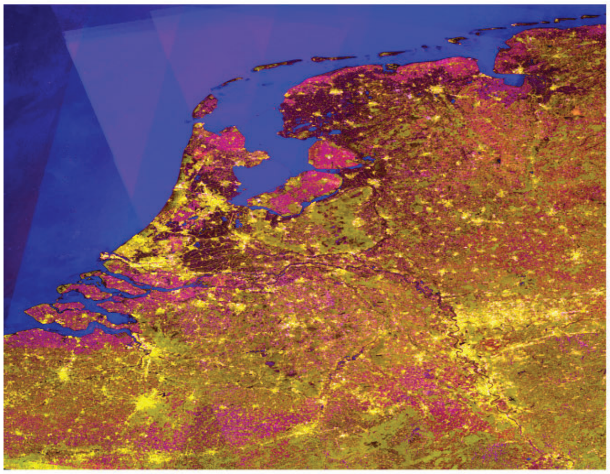

Figure 1. False color composite of average SAR backscatter (red), minimum SAR backscatter (green) and temporal variability of SAR backscatter (blue) for the Netherlands. SAR dataset: Envisat ASAR Wide Swath Mode.

3. SIGNATURE ANALYSIS

The combination of the minimum backscatter and the temporal variability makes water bodies unique when compared to other land cover types, as shown in Figure 1. The additional contribution of the average backscatter is marginal. The signatures of the multi-temporal SAR metrics minimum backscatter and temporal variability are shown in Figure 2 in form of density plots for different land cover types. The multi-temporal metrics were computed from the Envisat ASAR data with 300 m pixel size. The reference for the land cover was the Corine land cover 2006 product (http://sia.eionet.europa.eu/CLC2006) with a spatial resolution of 250 m and resampled to 300 m. The cluster of measurements of minimum backscatter and temporal variability of water surfaces is clearly separated from the cluster of measurements in correspondence of other land cover types. The behavior of the two multi-temporal SAR metrics shown in Figure 2 for the Netherlands was consistent among the six study areas (Table 1). Confusion with other land cover types occurred only when the number of backscatter measurements used for the computation of the temporal variability was below 10 or the area was characterized by a slope greater than 10 degrees.

The example in Figure 2 refers to pure "water" or "land" pixels. In case of pixels located along the edge between water and land, the metrics present a transition between the two clusters typical for "water" and "land" surfaces. Figure 3 shows an example for the study area of Andalusia. An analysis of the transition zone in terms of percentage of water fraction within a pixel revealed a slight trend of the metrics reaching from the "land" cluster to the "water" cluster for increasing water fraction. Water fraction was derived by superimposing the perimeter of a pixel onto high resolution images in Google Earth. Geolocation errors were taken into account by perturbating the location of the box with a white noise term based on the SAR image geocoding statistics. Typical geolocation errors were between 0.1 and 0.3 of the SAR pixel size.

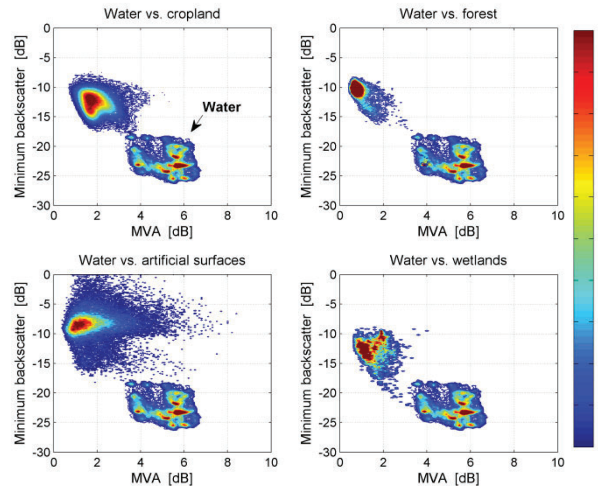

Figure 2. Density plots of temporal variability (referred to as MVA, mean annual variability) and minimum backscatter for “water” pixels with respect to other land cover classes according to the Corine land cover product for the Netherlands. The density plot for the “water” areas is shown in each plot for clarity reasons. The color bar on the right hand-side indicates increase of density from blue to red.

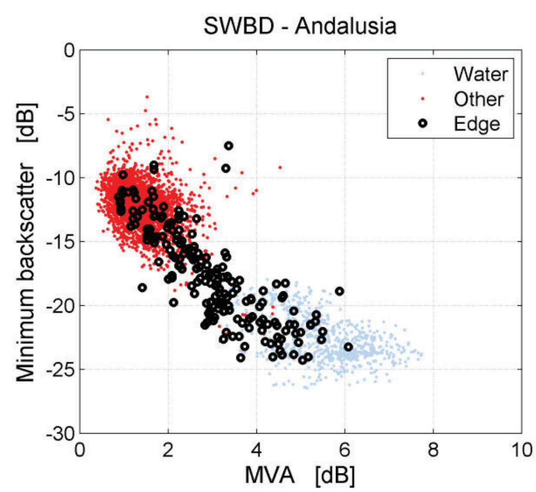

Figure 3. Scatterplot of temporal variability (MVA) and minimum backscatter for the study area of Andalusia. Measurements have been grouped according to the class they belong to in the SRTM Water Body Dataset (SWBD) (“water”, “other”). Pixels located along a coastline have been further differentiated ("edge") regardless of the land cover type.

4. WATER BODIES CLASSIFICATION APPROACH

The signature analysis suggested that a simple decision algorithm based on where a pair of measurements of temporal variability and minimum backscatter is located in the feature space is sufficient to obtain reasonable separation between water and land. Figure 4 gives a graphic representation of the water body detection algorithm. The black line separates the parts of the feature space where "land" and "water" pixels are supposed to fall. In addition, it is assumed that temporal variability below 1.5 dB cannot represent a water surface. Similarly, a minimum backscatter above -16 dB is not realistic for water. The equation for the line separating the feature space is

$$y = 3.5 \cdot x - 28 \qquad (1)$$

where x represents the temporal variability in dB and y the minimum backscatter in dB. The two coefficients in Equation (1) correspond to the best classification results for the area of the Netherlands. When then used for the remaining study areas, they still provided among the best classification results.

To avoid mis-classifications, pixels for which the temporal variability is based on less than 10 backscatter measurements are not classified. In addition, pixels labeled as "water: but located on slopes greater than 10 degrees are re-labeled as "land". Slope angle was derived from the SRTM-3 Digital Elevation Model dataset (http://srtm.csi.cgiar.org/). The dataset of 3-arcsecond Russian topographic maps for Eurasia (http://www.viewfinderpanoramas.org/) was used for areas located north of 60° N. The elevation datasets were multi-looked within a 3×3 window to decrease local noise.

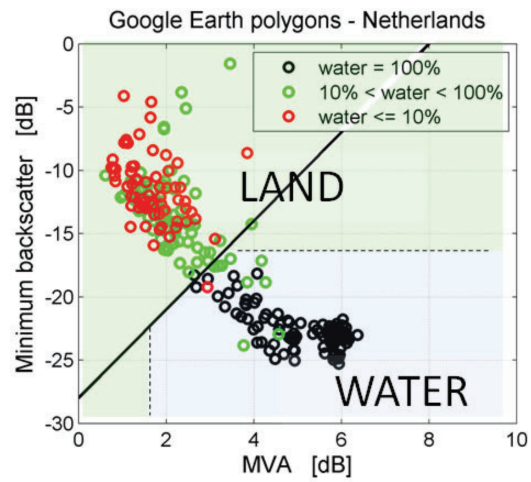

Figure 4. Illustration of water detection algorithm. The black line represents Equation (1). Additional decision rules are represented by the dashed lines. The "water" and the "land" areas resulting from the decision rules are colored in light blue and green, respectively. The decision rules are super-imposed on a set of sample measurements (circles) of temporal variability (MVA) and minimum backscatter. The water fraction in correspondence of each sample was estimated from high resolution imagery in Google Earth. Number of samples: 279.

5. WATER BODIES CLASSIFICATION RESULTS

Figure 5 shows the water body maps for the Netherlands obtained from the ASAR data at 75 m, 150 m and 300 m. For decreasing spatial resolution, delineation of the water bodies becomes poorer and water bodies of the size of a pixel (e.g., rivers) tend to disappear.

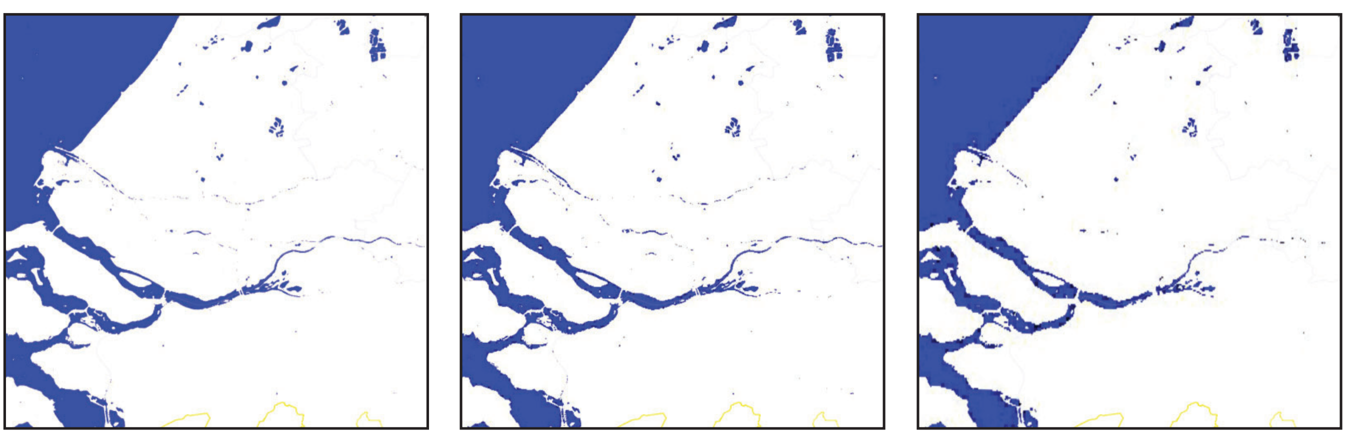

(a) (b) (c)

Figure 5. Water body maps derived from Envisat ASAR WSM data at 75 m (a), 150 m (b) and 300 m, for a portion of the Netherlands study area.

Table 2. Classification accuracy of water body detection for the study area of the Netherlands (UA: User's accuracy; PA: Producer's accuracy; OA: Overall accuracy).

	UA water	UA land	PA water	PA land	OA
Google Earth	100.0	88.0	90.8	100.0	94.5
	98.6	91.4	88.7	99.0	94.3
CLC2006	97.8	98.4	82.2	99.5	98.4
	98.3	98.3	80.3	99.9	98.3

Table 2 shows the classification accuracy in terms of user's, producer's and overall accuracy (UA, PA and OA respectively) for the Netherlands. The accuracy was assessed against polygons selected in Google Earth (300 samples) and the Corine Land Cover (CLC2006) product (no sampling). For each dataset, the two rows correspond to the comparison at 150 m and 300 m, respectively. Similar results were obtained at all six study areas. The classification accuracy was typically on the order of 90% or above and indicated slightly better performance when starting from the 150 m SAR data. Slightly lower accuracies where obtained for the water class in terms of omission errors in consequence of small water bodies that were not correctly delineated in the SAR dataset.

6. CONCLUSIONS

In this study we looked at the potential of C-band SAR multi-temporal metrics to detect water bodies. The combination of the backscatter temporal variability and the minimum backscatter proved to be reliable for separating water bodies from other land cover types. Tests were carried out at six study areas with different types of water bodies and land cover. Detection of pure "water" and "land" pixels with a simple thresholding algorithm was found to be almost error-free. Some ambiguity was noticed in case of mixed pixels with a water fraction. Higher resolution improved some of the details but did not lead to substantially different results, in particular concerning the delineation of the water bodies.

The availability of repeated acquisitions of Envisat ASAR Wide Swath Mode data on a global scale and the results here reported indicate that such a straightforward approach can be used to generate a global water body dataset. Adaptation of the temporal extent of the window size within which the multi-temporal metrics are computed can further serve the purpose of labeling a water body as permanent or temporary.

7. ACKNOWLEDGMENTS

This study was supported by European Space Agency (ESA) within the Climate Change Initiative Land Cover (CCI-LC) Project. P. Defourny, S. Bontemps and J. Radoux, UCL, are acknowledged for scientific advice. Envisat ASAR data have been acquired and distributed under ESA's Category-1 project nr. 8073.

8. REFERENCES

[1] A. Bartsch, R. Kidd, C. Pathe, W. Wagner, and K. Scipal, "Satellite radar imagery for monitoring inland wetlands in boreal and sub-arctic environments," Journal of Aquatic Conservation: Marine and Freshwater Ecosystems, vol. 17, pp. 305-317, 2007.

[2] U. Wegmüller and C. Werner, "Retrieval of vegetation parameters with SAR interferometry," IEEE Trans. Geosci. Remote Sensing, vol. 35, pp. 18-24, 1997.

[3] U. Wegmüller, "Automated terrain corrected SAR geocoding," Proc. IGARSS'99, Hamburg, 28 June - 2 July, 1999.

[4] S. Quegan and J. J. Yu, "Filtering of multichannel SAR images," IEEE Trans. Geosci. Remote Sensing, vol. 39, pp. 2373-2379, 2001.

[5] A. Wiesmann, U. Wegmüller, M. Santoro, T. Strozzi, and C. Werner, "Multi-temporal and multi-incidence angle ASAR Wide Swath data for land cover information," Proc. 4th International Symposium on Retrieval of Bio- and Geophysical Parameters from SAR Data for Land Applications, Innsbruck, 16-19 November, 2004.